

AFRL-ML-WP-TP-2007-464

**A MODEL FOR THE OXIDATION OF
REFRACTORY DIBORIDES
(PREPRINT)**

T.A. Parthasarathy, Ronald J. Kerans, and M. Opeka



MAY 2007

Approved for public release; distribution unlimited.

STINFO COPY

The U.S. Government is joint author of this work and has the right to use, modify, reproduce, release, perform, display, or disclose the work.

**MATERIALS AND MANUFACTURING DIRECTORATE
AIR FORCE RESEARCH LABORATORY
AIR FORCE MATERIEL COMMAND
WRIGHT-PATTERSON AIR FORCE BASE, OH 45433-7750**

REPORT DOCUMENTATION PAGE

Form Approved
OMB No. 0704-0188

The public reporting burden for this collection of information is estimated to average 1 hour per response, including the time for reviewing instructions, searching existing data sources, gathering and maintaining the data needed, and completing and reviewing the collection of information. Send comments regarding this burden estimate or any other aspect of this collection of information, including suggestions for reducing this burden, to Department of Defense, Washington Headquarters Services, Directorate for Information Operations and Reports (0704-0188), 1215 Jefferson Davis Highway, Suite 1204, Arlington, VA 22202-4302. Respondents should be aware that notwithstanding any other provision of law, no person shall be subject to any penalty for failing to comply with a collection of information if it does not display a currently valid OMB control number. **PLEASE DO NOT RETURN YOUR FORM TO THE ABOVE ADDRESS.**

1. REPORT DATE (DD-MM-YY) May 2007		2. REPORT TYPE Journal Article Preprint		3. DATES COVERED (From - To) N/A	
4. TITLE AND SUBTITLE A MODEL FOR THE OXIDATION OF REFRACTORY DIBORIDES (PREPRINT)				5a. CONTRACT NUMBER FA8650-04-D-5233	
				5b. GRANT NUMBER	
				5c. PROGRAM ELEMENT NUMBER 62102F	
6. AUTHOR(S) T.A. Parthasarathy (UES, Inc.) Ronald J. Kerans (AFRL/MLLN) M. Opeka (Naval Surface Warfare Center)				5d. PROJECT NUMBER 2311	
				5e. TASK NUMBER 00	
				5f. WORK UNIT NUMBER 23110002	
7. PERFORMING ORGANIZATION NAME(S) AND ADDRESS(ES) UES Inc. 4401 Dayton-Xenia Road Dayton, OH 45432-1894				8. PERFORMING ORGANIZATION REPORT NUMBER	
Ceramics Branch (AFRL/MLLN) Metals, Ceramics & Nondestructive Evaluation Division Materials and Manufacturing Directorate Air Force Research Laboratory, Air Force Materiel Command Wright-Patterson Air Force Base, OH 45433-7750 ----- Naval Surface Warfare Center Caderock, MD					
9. SPONSORING/MONITORING AGENCY NAME(S) AND ADDRESS(ES) Materials and Manufacturing Directorate Air Force Research Laboratory Air Force Materiel Command Wright-Patterson AFB, OH 45433-7750				10. SPONSORING/MONITORING AGENCY ACRONYM(S) AFRL-ML-WP	
				11. SPONSORING/MONITORING AGENCY REPORT NUMBER(S) AFRL-ML-WP-TP-2007-464	
12. DISTRIBUTION/AVAILABILITY STATEMENT Approved for public release; distribution unlimited.					
13. SUPPLEMENTARY NOTES Journal article submitted to Acta Materialia. The U.S. Government is joint author of this work and has the right to use, modify, reproduce, release, perform, display, or disclose the work. PAO Case Number: AFRL/WS 07-0233, 05 Feb 2007. Paper contains color content.					
14. ABSTRACT Hypersonic applications require materials that can withstand very high temperatures. Refractory diborides appear to be the most promising candidates for these applications, from the standpoint of resistance to oxidation and evaporative loss. In this work, a mechanistic model is presented that predicts the oxidation behavior of diborides of Zr, Hf and Ti. Using available thermodynamic data and literature data on vapor pressures, good correspondence is obtained between theory and experiments for weight gain, recession and scale thickness as a function of temperature and oxygen partial pressure.					
15. SUBJECT TERMS Oxidation; Refractory Diborides					
16. SECURITY CLASSIFICATION OF:			17. LIMITATION OF ABSTRACT: SAR	18. NUMBER OF PAGES 30	19a. NAME OF RESPONSIBLE PERSON (Monitor) Ronald J. Kerans
a. REPORT Unclassified	b. ABSTRACT Unclassified	c. THIS PAGE Unclassified			

Standard Form 298 (Rev. 8-98)
Prescribed by ANSI Std. Z39-18

A model for the oxidation of refractory diborides

T A Parthasarathy*, R J Kerans, M Opeka^

Air Force Research Laboratory,

Materials and Manufacturing Directorate, AFRL/MLLN,

Wright-Patterson AFB, OH 45433-7817

* UES, Inc., Dayton OH 45432

^Naval Surface Warfare center, Caderock, MD

Abstract

Hypersonic applications require materials that can withstand very high temperatures. Refractory diborides appear to be the most promising candidates for these applications, from the standpoint of resistance to oxidation and evaporative loss. In this work, a mechanistic model is presented that predicts the oxidation behavior of diborides of Zr, Hf and Ti. Using available thermodynamic data and literature data on vapor pressures, good correspondence is obtained between theory and experiments for weight gain, recession and scale thickness as a function of temperature and oxygen partial pressure.

1.0 Introduction

The leading edge of a hypersonic vehicle is subjected to very high temperatures and has to survive the flight without losing the integrity of the leading edge geometry along the span.^{1,2} The high temperatures and the low pressure environment make oxidation and evaporative loss critical factors in material choice.³ The diborides of refractory metals (esp., Zr and Hf), which are termed ultra-high temperature ceramics (UHTC) have high melting points and are the most promising among known materials that are likely to survive for long-term use under hypersonic conditions.^{3,4} The diborides

are also attractive due to their higher thermal conductivity which will be required to offset the stringent thermal gradients imposed by the aerothermal effects of hypersonic conditions.

The history of work on oxidation of diborides is given by Opeka et al.³ After the promise shown from early works, a good screening study of refractory element diborides was conducted and reported by Fenter.⁵ He reported the diborides of Zr and Hf to be the most oxidation resistant of the diborides. He further reported that additions of SiC up to 20% by volume further improved the oxidation resistance of these materials. It has been pointed out by Opeka et al.^{3,4,6} that the high melting point and low vapor pressures of the oxides and sub-oxides of Zr and Hf are responsible for the superior high temperature resistance of these materials. Using volatility diagrams, they further point out that of the various possible high melting compounds of Zr, and Hf, the borides appear to have the least issues with respect to disruption of the scale formation. In carbides, CO vapor pressures exceed 1 atm above 1730C, and in silicides, the active oxidation to gaseous SiO disrupts the scale above 1800C. In contrast, the boric oxide is glassy, flows to fill porous oxide scale, allowing evaporation of the oxide to take place without breaking up the scale. When SiC is added to the system, further improvements are possible since the silica based glass offers greater resistance to evaporation than B₂O₃ alone.⁷

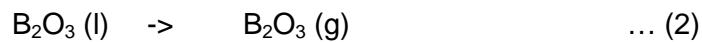
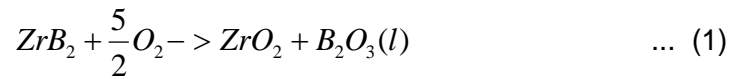
Thus far understanding of the superior oxidation behavior of the diborides has been qualitative. For engineering design and application, a quantitative model that predicts all aspects of oxidation is desired. It is desirable to have predictions under a set of complex conditions of temperature and environment of factors such as scale thickness, metal recession and weight change. Many experimental work have been under isothermal conditions and in laboratory environment, while real engineering conditions will involve thermal gradients and environmental gradients.

A model that can be applied to engineering conditions is the long-term objective of this work. However the complex nature of the materials make it necessary to start with a model for the simpler systems and conditions, where reliable experimental data under well known conditions are available. In this paper, we present a model that is found to predict the scale thickness, metal recession and weight changes for diborides of Zr, Hf, and Ti under isothermal conditions. Various factors such as residual boron content and dependences on temperature and oxygen partial pressures are also predicted and found to be in reasonable agreement with experiments. It is suggested that this model provides a reasonable basis for future work.

2.0 Conceptual framework

The model reported in this work is based on concepts of the oxidation process derived from microstructural details available in the literature. The morphology of the oxidation product as well as the phase present and their distribution have been reported on by several works. For the case of ZrB_2 (and HfB_2), oxidation in air at temperatures of up to $1300^\circ C$ results in a dense adherent oxide scale. The scale consists of a ZrO_2 and B_2O_3 , and no intermediate phases have been observed at the interfaces. The top surface of the scale is nodular ZrO_2 , and the cross-section reveals more columnar structure of ZrO_2 with glassy B_2O_3 in-between the columnar grains. At lower temperatures ($<1100^\circ C$) a glassy B_2O_3 is observed on top of the ZrO_2 scale, but is absent above $1300^\circ C$. The microstructure of the ZrO_2 appears to change from equiaxed grains at temperatures below $1100^\circ C$, to columnar at higher temperatures. This transition temperature is $\sim 1650^\circ C$ for HfB_2 . Similar transition has been noted with respect to oxygen partial pressure. The oxygen partial pressure dependence changes from linear to no dependence as temperature is increased above $1150^\circ C$.

Based on the above observations, the following conceptual framework is suggested. A schematic sketch is shown in Fig.1. Oxidation of the refractory element results in an evaporation resistant refractory oxide which forms a porous skeleton. The oxidation of boron results in a glassy boric oxide that flows to fill the porous skeleton. At the surface the boria evaporates. At steady state the oxidation takes place through gaseous diffusion of oxygen through the pores in the oxide skeleton, continuing to diffuse through the liquid boria (that fills the porous skeleton beneath the surface) to reach the ZrB_2 oxide scale interface. The two rate limiting reactions are



The rate of dissolution of oxygen in B_2O_3 is taken not to be rate-limiting in the model developed below. The permeation of oxygen through the refractory oxide is assumed to be negligible compared to that through the pores filled with glassy boria.

3.0 The Model

The objective of the model is to predict the kinetics of scale thickness, substrate recession and weight change as a function of time at temperature and oxygen partial pressure. A schematic of the model is shown in Fig.2.

The ambient air is taken to consist of N_2 and O_2 only. A small fraction, f_c , of the scale is taken to be porous and provide a continuous pathway for liquid B_2O_3 to pass through and evaporate at the surface, which is taken to be a perfect sink for B_2O_3 . The relative kinetics of filling of the pore by oxidation at the scale/substrate interface and the evaporation at the surface of B_2O_3 determines the extent to which the pores are filled with B_2O_3 . At a given time, t , the scale has a thickness of L and the inner portion of the scale is filled with liquid B_2O_3 to a thickness, h . The distance $(L-h)$ is the diffusion

distance over which gaseous oxygen must diffuse to get to the B₂O₃. The oxygen is taken to dissolve in B₂O₃ and continue to diffuse to the substrate/scale interface. The oxide scale itself is taken to be impervious to oxygen (due to its low electrical conductivity).

At the scale/substrate interface, reaction 1 takes place. Thus, at steady state, the flux of oxygen must be balanced by the formation rates of ZrO₂ and B₂O₃.

$$J_{O_2} = \frac{5}{2} J_{B_2O_3} = \frac{5}{2} J_{ZrO_2} \quad \dots (3)$$

The flux of oxygen down the porous channel that is (L-t) in length is given by :

$$J_{O_2} = D_{O_2} \frac{C_{O_2}^a - C_{O_2}^i}{L-h} f_c \quad \dots (4)$$

In the above equation, D refers to diffusion coefficient, C refers to concentration, subscript O₂ refers to oxygen, and superscript "i" refers to the interface between B₂O₃ (l) and B₂O₃(v), which is at a distance t from the substrate/scale interface. Similarly the flux of B₂O₃(v) from the surface of B₂O₃(l) to the ambient, is given by :

$$J_{B_2O_3} = D_{B_2O_3} \frac{C_{B_2O_3}^i - C_{B_2O_3}^a}{L-h} f_c \quad \dots (5)$$

Combining equations (3), (4) and (5) the oxygen concentration at the B₂O₃ liquid vapor interface is obtained as :

$$C_{O_2}^i = C_{O_2}^a - \frac{5 D_{B_2O_3}}{2 D_{O_2}} (C_{B_2O_3}^i - C_{B_2O_3}^a) \quad \dots (6)$$

The concentration, $C_{B_2O_3}^a$, at the ambient surface is taken to be zero. The concentration, $C_{B_2O_3}^i$, of the B₂O₃(v) at this interface is obtained from vapor pressure data. ⁸

$$C_{B_2O_3}^i = \frac{P_{B_2O_3}}{RT}; \quad P_{B_2O_3} = 3 \times 10^{10} \exp\left(-\frac{45,686}{T}\right) atm \quad \dots (7)$$

The permeability of oxygen through the liquid B₂O₃ depends on the oxygen partial pressures across the liquid layer of thickness t. The oxygen partial pressure at the B₂O₃ liquid-vapor interface is given by,

$$P_{O_2}^i = RT C_{O_2}^i \quad \dots (8)$$

The partial pressure of oxygen at the scale B₂O₃ interface is given by,

$$K_{reaction1} = \frac{a_{ZrB_2} P_{O_2}^{5/2}}{a_{B_2O_3} a_{ZrO_2}} \quad \dots (9)$$

Using the thermodynamic data of Barin⁸ for reaction 1, equation (9) gives the following for the oxygen partial pressure, $P_{O_2}^{i2}$, at the ZrB₂-B₂O₃ interface (i2).

$$P_{O_2}^{i2} = 5 \times 10^{10} \exp\left(-\frac{99967}{T}\right) atm \quad \dots (10)$$

The values given by equation (10) are consistent with the maps presented by Fahrenholtz.⁹ Diffusivity of oxygen through boria has been measured by Tokuda et al., who found a linear dependence on oxygen partial pressure and deduced that it diffuses as molecular oxygen. The oxygen flux, $J_{O_2(B_2O_3)}$, across the liquid boria is related to the partial pressure gradient through oxygen permeability coefficient,^{10,11} as:

$$J_{O_2(B_2O_3)} = \frac{P_{O_2-B_2O_3}}{h} f_c [P_{O_2}^i - P_{O_2}^{i2}] \quad \dots (11)$$

The oxygen permeability coefficient, $P_{O_2-B_2O_3}$, is obtained from the literature^{11,12}, as:

$$P_{O_2-B_2O_3} = 7 \times 10^{-3} \exp\left(\frac{-14000}{T}\right) mole/m-s-atm \quad \dots (12)$$

Combining equations 11 and 12 and equating to the flux of oxygen through the gaseous layer, given by equation 4, an equation relating the boria layer thickness, t, to the scale thickness, L, is obtained.

$$h = qL \quad ; \quad q = \frac{P_{O_2-B_2O_3}(P_{O_2}^i - P_{O_2}^{i2})}{D_{O_2}(C_{O_2}^a - C_{O_2}^i) + P_{O_2-B_2O_3}F(P_{O_2}^i)} \quad \dots (13)$$

The equations for the rate of change of scale thickness and mass of the scale are given by accounting for mass balance and equation 3.

$$\frac{dL}{dt} = \frac{1}{1-f_c} \frac{dW_{ZrO_2}}{dt} \frac{1}{\rho_{ZrO_2}} = \frac{1}{1-f_c} \frac{2}{5} J_{O_2} \frac{M_{ZrO_2}}{\rho_{ZrO_2}} \quad \dots (14)$$

Combining with equation 4, one obtains:

$$\frac{dL}{dt} = \frac{2}{5} \frac{M_{ZrO_2}}{\rho_{ZrO_2}} D_{O_2} \frac{C_{O_2}^a - C_{O_2}^i}{L(1-q)} \frac{f_c}{1-f_c} \quad \dots (15)$$

Integration of equation 15 gives the parabolic growth equation for scale thickness.

$$L^2 = 2 \left[\frac{2}{5} \frac{M_{ZrO_2}}{\rho_{ZrO_2}} D_{O_2} \frac{C_{O_2}^a - C_{O_2}^i}{(1-q)} \frac{f_c}{1-f_c} \right] t \quad \dots (16)$$

The recession of the substrate is given by

$$R = L(1-f_c) \frac{M_{ZrB_2} / \rho_{ZrB_2}}{M_{ZrO_2} / \rho_{ZrO_2}} \quad \dots (17)$$

The total weight change per unit area is given by:

$$\frac{\Delta m}{A} = L \rho_{ZrO_2} (1-f_c) + h f_c \rho_{B_2O_3} - R \rho_{ZrB_2} \quad \dots (18)$$

It remains to obtain expressions for the diffusion coefficient of oxygen through the porous region filled with oxygen, $B_2O_3(v)$ and nitrogen. The diffusion coefficient in a multicomponent gaseous system can be approximated by:¹³

$$D_{1,(2,..,i)} = \frac{1}{\sum_{i \neq 1} (x_i / D_{1-i})} \quad ; \quad x_i = \frac{n_i}{\sum_{j \neq 1} n_j} \quad \dots (19)$$

Where D refers to diffusivity, n to mole fraction, subscript "1, (2,,i)" refers to the diffusivity of specie 1 in a medium of i species, subscript "1-i" refers to diffusivity of specie 1 in a binary mixture of species 1 and i. The diffusivity, D_{1-2} , of specie 1 in a binary gas mixture with specie 2, is given by¹⁴

$$D_{1-2} = \frac{0.0018583T^{3/2}\sqrt{(1/M_1) + (1/M_2)}}{Pr_{12}^2 \Omega_D} \quad \dots (20)$$

where D_{1-2} = gas diffusivity in cm^2/sec

$$\Omega_D = \frac{1.06036}{T^{*0.15610}} + \frac{0.193000}{\exp(0.47635T^*)} + \frac{1.03587}{\exp(1.52996T^*)} + \frac{1.76474}{\exp(3.89411T^*)}$$

$$T^* = \frac{kT}{\varepsilon_{12}}, \varepsilon_{12} = \sqrt{\varepsilon_1 \varepsilon_2}, r_{12} = 0.5(r_1 + r_2) \text{ in Angstroms, } P = \text{pressure in atm,}$$

M_i = molecular weight (gms/mole)

The parameters needed for the above expressions can be obtained from the work of Svehla.¹⁵ When the size of the pore is small, the diffusivity of the gases is determined by Knudsen diffusivity. This is given by¹⁶:

$$D_k = \frac{4}{3} \left(\frac{8RT}{\pi M} \right)^{1/2} \frac{r}{2} \quad \dots (21)$$

where D_k is the Knudsen diffusivity, M the molecular mass of the diffusing species, and r the radius of the porous pathway. The effective diffusivity is given by¹⁶:

$$D_{eff} = (D_k^{-1} + D_{1-2}^{-1})^{-1} \quad \dots (22)$$

Using the expressions, 19 through 22, Equations 16 through 18 give the scale thickness, recession and weight gain as a function of temperature, time and partial pressure of oxygen.

4.0 Model Predictions compared with literature data

4.1 ZrB_2

The model was verified by comparing with experimental data reported in the literature for ZrB_2 . Extensive TGA data on weight change versus time in 250Torr of pure oxygen has been reported by Tripp and Graham.¹⁷ They also compare their results with the parabolic rate constant data from prior work by Berkowitz¹⁸ and Kuraikose and Margrave.¹⁹ Figure 3 shows their results compared with the model predictions, for an assumed pore fraction of 0.05 and pore radius of 0.5 micron. The model predictions for the weight change with time are shown for three different temperatures in Figure 3(a), while the parabolic rate constants are shown plotted in Fig3(b). The data of Tripp and Graham deviates from the model at temperatures above 1200C. However when the model is compared with all of the reported data, the correspondence is good.

A study by Fenter reported on the metal recession of several diborides in air, as a function of temperature.⁵ The results on ZrB_2 is shown in Figure 4(a) along with the model predictions. The model compares very well with data upto ~1850C. Above this temperature, the model predicts that all of the boride will evaporate as soon as it forms. The experimental data shows a significant enhancement in recession at this temperature. The model predicts the transition temperature correctly, but not the upward trend in recession. It is not clear if there was significant spallation in the experiments above this temperature.

Finally, recent works by Opeka et al.^{3,6} and Talmy et al.²⁰ have reported on mass change and oxide layer thicknesses of ZrB_2 in air or Ar/O₂ mixtures. Their data are

shown compared with the model predictions in Figure 4 (b) and (c). The correspondence is seen to be good. The choice of pore fraction and radius were kept the same for all of the model predictions.

4.2 HfB₂

The model is easily extended to other diborides by simply using the appropriate thermodynamic data and the appropriate physical properties such as molecular weight, density, etc. For HfB₂, one obtains the oxygen partial pressure, $P_{O_2}^{i2}$, at the HfB₂-B₂O₃ interface as

$$P_{O_2}^{i2(Hf)} = 6 \times 10^9 \exp\left(-\frac{100070}{T}\right) atm \quad \dots \quad (23)$$

There have been two reports in the literature that have characterized the oxidation behavior of HfB₂. Fenter⁵ has measured the recession rates in air, while Berkowitz¹⁸ has reported on the parabolic rate constants in 250Torr of pure oxygen. These data are compared with the model predictions using a pore fraction of 0.05 and pore radius of 0.5 micron in Figure 5. The predicted recession is higher than the measured values, while the predicted parabolic rate constants are lower.

4.3 TiB₂

For TiB₂, one obtains the oxygen partial pressure, $P_{O_2}^{i2}$, at the TiB₂-B₂O₃ interface as

$$P_{O_2}^{i2(Hf)} = 5 \times 10^{10} \exp\left(-\frac{95126}{T}\right) atm \quad \dots \quad (24)$$

Using the appropriate physical properties for TiO_2 and TiB_2 the oxidation behavior was predicted, once again assuming a pore fraction of 0.05 and a pore radius of 0.5 micron. The predictions were evaluated by comparing with experimental data available on weight change and recession as reported by Koh et al.²¹ This comparison is shown in Figure 6.

5.0 Parametric/sensitivity studies

A parametric study was conducted to assess model sensitivity and to determine the effects of experimental variables. Figure 7 shows the temperature dependence of the parabolic rate constant in ZrB_2 . A clear change in apparent activation energy is seen at around 1400C. The figure includes the prediction fraction of boria in the scale. It is clear that the change in activation energy arises from the loss of boria from the scale.

Next, the model was used to study the effect of varying the pore fraction and pore radius, to assess its sensitivity. These parameters are difficult to measure and have not been reported experimentally. Further, since the model assumes neglects the tortuosity of the porous scale, the pore radius and and pore fraction used in the model must be considered to be "effective" parameters rather than the actual physical values. It is quite possible that these parameters themselves vary with temperature or other experimental conditions such as environment. Thus it is useful to conduct a sensitivity study.

Figure 8 shows the effect of pore radius on the recession, scale thickness, parabolic rate constant and the fraction of boria in the scale. It is found that the effect is significant when the pore radius is smaller than about 1 micron. Further, the effect is insignificant at temperatures below about 1400C, which corresponds to the temperature where boria evaporation becomes significant.

Figure 9 shows the effect of pore fraction on the oxidation behavior of ZrB_2 in air. The rate constant, scale thickness and recession all increase by about an order of

magnitude when the pore fraction is increased from 0.025 to 0.2. Thus the effect is nearly linear.

Figure 10a summarizes the effect of oxygen partial pressure on the parabolic rate constant as a function of temperature. The dependence is linear at 1000C and becomes independent at 1600C; this is consistent with the experimental observation of Berkowiz.¹⁸ Figure 10b shows that pore radius is predicted to have a significant effect at low oxygen partial pressures and the pore fraction has a near-linear effect as might be expected.

6.0 Summary

A physical model to predict the oxidation behavior of refractory diborides is presented. The model assumes that the refractory oxide is inert to oxygen diffusion due to lack of sufficient electrical conductivity. The porosity in the oxide is taken to be filled with liquid boria which evaporates from the surface. A comparison with experimental data in the literature shows that the steady state model is found to predict the weight change, metal recession, oxide scale thickness, the temperature dependence of the parabolic rate constant reasonably well for ZrB₂. Comparison with limited literature data on HfB₂ and TiB₂ show that the model may have a general applicability to refractory diborides, although data on electrical conductivity of the oxides especially at high temperatures will be required to refine the model.

7.0 Acknowledgments

It is a pleasure to acknowledge useful discussions with Prof. R. Rapp, of The Ohio State Univ. This work was supported in part by USAF Contract # FA8650-04-D-5233.

8.0 References

1. R. Savino, M.D.S. Fumo, D. paterna, and M. Serpico, "Aerothermodynamic study of UHTC-based thermal protection systems," *Aerospace Sci and Tech.*, **9** 151-160 (2005).
2. I.D. Boyd, and J.F. Padilla, "Simulation of sharp leading edge aerothermodynamics," *AIAA*, **2003-7062** 1-10 (2003).
3. M.M. Opeka, I.G. Talmy, and J.A. Zaykoski, "Oxidation-based materials selection for 2000C+ hypersonic aerosurfaces: Theoretical considerations and historical experience," *J. Mater. Sci.*, **39** 5887-5904 (2004).
4. E. Wuchina, M. Opeka, S. Causey, K. Buesking, J. Spain, A. Cull, J. Routbort, and F. Guitierrez-Mora, "Designing for ultrahigh-temperature applications: The mechanical and thermal properties of HfB₂, HfCx, HfNx and a-Hf(N)," *J. Mater. Sci.*, **39** 5939-5949 (2004).
5. J.R. Fenter, "Refractory diborides as engineering materials," *SAMPE Quarterly*, **2,3** [1-15] (1971).
6. M.M. Opeka, I.G. Talkmy, E.J. Wuchina, J.A. Zaykoski, and S.J. Causey, "Mechanical, thermal and oxidation properties of refractory hafnium and zirconium compounds," *Jl. Eur. Ceram. Soc.*, **19** 2405-2414 (1999).
7. S.R. Levine, E.J. Opila, M.C. Halbig, J.D. Kiser, M. Singh, and J.A. Salem, "Evaluation of ultra-high temperature ceramics for aeropropulsion use," *Jl Eur. Ceram. Soc.*, **22** 2757-2767 (2002).
8. I. Barin, VCH Verlagsgesellschaft., New York, (1995).
9. W.G. Fahrenholtz, "The ZrB₂ volatility diagram," *J. Amer. Ceram. Soc.*, **88** [12] 3509-3512 (2005).
10. E.L. Courtright, "Ultrahigh temperature composite assessment study - Carbon/Carbon," *US Air Force Tech. Report WL-TR-92-4009* (1992).
11. K.L. Luthra, "Oxidation of Carbon/Carbon composites - A theoretical analysis," *Carbon*, **26** 217-224 (1988).
12. T. Tokuda, T. Ido, and T. Yamaguchi, *Z Naturforschung*, **26A** 2058-2060 (1971).
13. R.J. Wetty, C.E. Wicks, and R.E. Wilson, John Wiley & sons, NY, (1984).
14. R.B. Bird, W.E. Stewart, and L.E. N, J Wiley & Sons, New York, USA, (2002).
15. R.A. Svehla, "Estimated viscosities and thermal conductivities of gases at high temperatures" (NASA Tech report R-132, 1962).
16. J. Szekely, J.W. Evans, and H.Y. Sohn, "Gas Solid Reactions", Academic Press, New York, (1976).
17. W.C. Tripp, and H.C. Graham, "Thermogravimetric study of the oxidation of ZrB₂ in the temperature range of 800 to 1500 C," *J. Electrochem. Soc.*, **118** [7] 1195-1199 (1971).
18. J.B. Berkowitz-Mattuck, *J. Electrochem. Soc.*, **113** 908 (1966).
19. A.K. Kuriakose, and J.L. Margrave, *J. Electrochem. Soc.*, **111** 827 (1964).
20. I. Talmy, J. Zaykoski, M. Opeka, and A. Smith, "Oxidation of ZrB₂ ceramics containing SiC, TaSi₂, Ta₅Si₃ and Si₃N₄ as silica formers in oxidized surface layer," *Oxidation Modeling workshop, Washington DC* (2005).
21. Y.-H. Koh, S.-Y. Lee, and H.-E. Kim, "Oxidation behavior of titanium boride at elevated temperatures," *J. Amer. Ceram. Soc.*, **54** [1] 229-241 (2001).

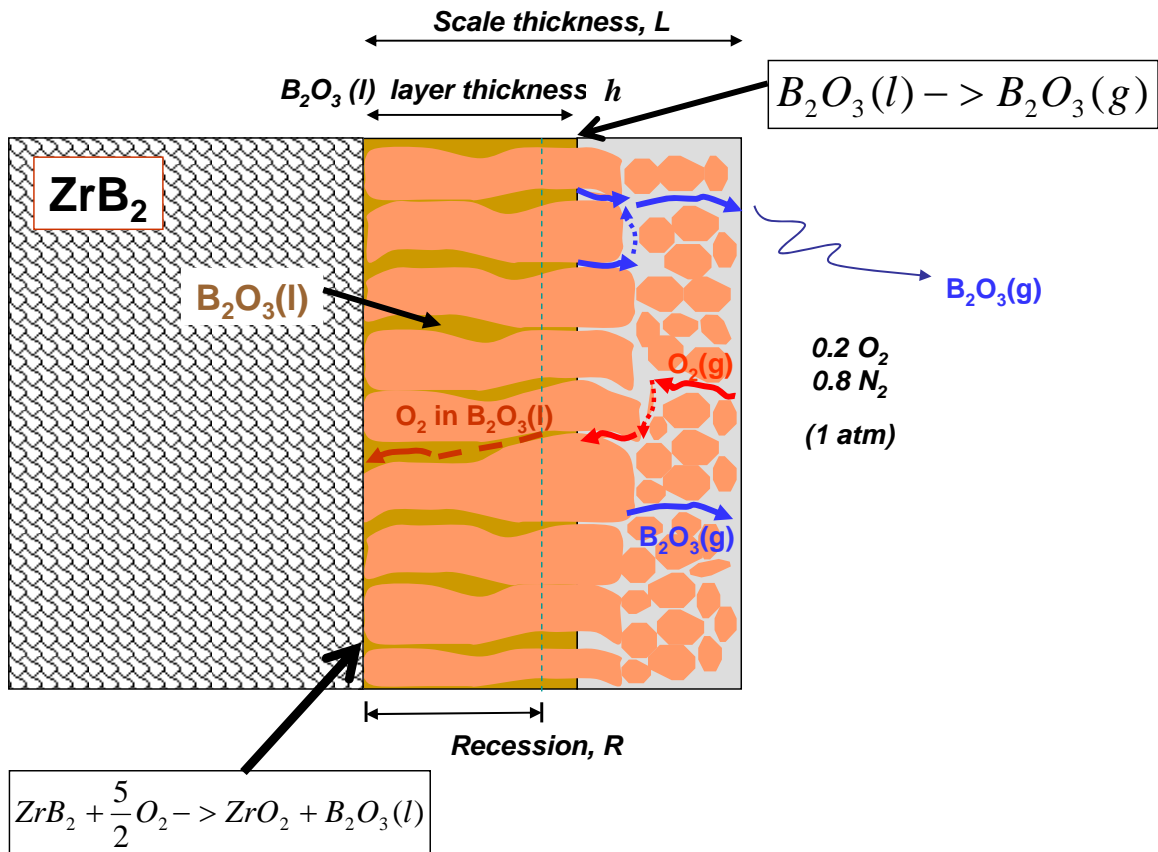


Figure 1 Schematic sketch of mechanisms involved in the oxidation of ZrB_2 in air, that were assumed in the model.

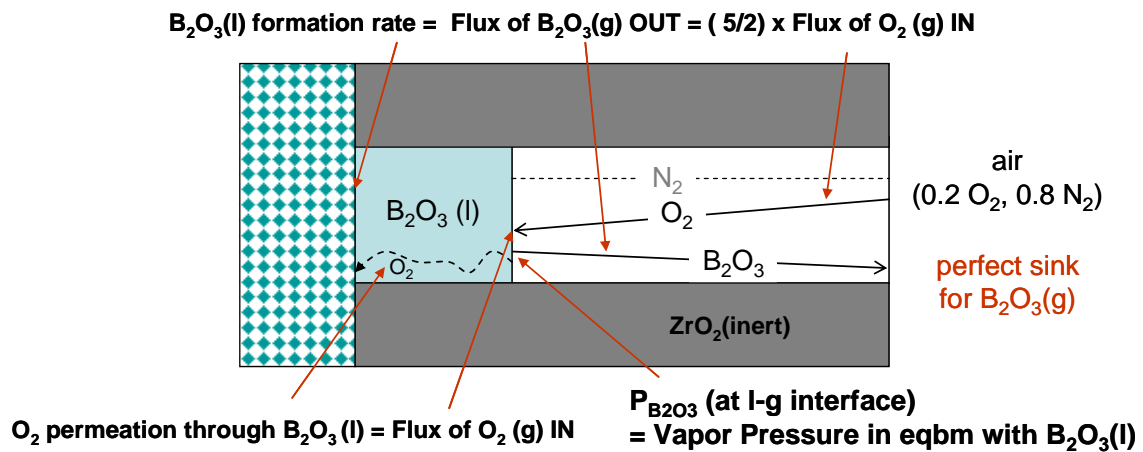


Figure 2 A schematic sketch of the steps involved in the oxidation of ZrB_2 , that were considered in the model. The ZrO_2 is taken to be inert to oxygen permeation. The porous region within the ZrO_2 is assumed to be continuous and tortuosity is neglected. The pores were taken to be filled with the oxidation product, liquid boria, which is lost partially by evaporation through the porous region. At steady state the porous region is partially filled with boria.

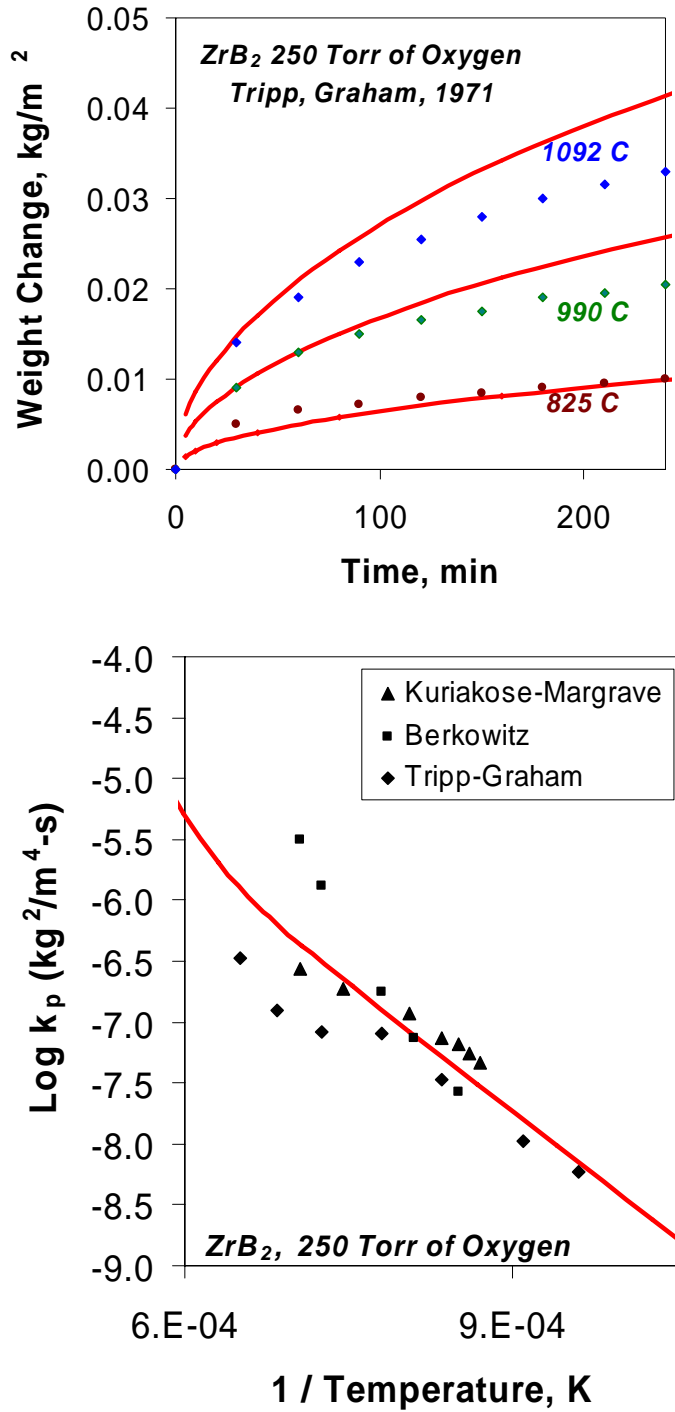


Figure 3 (a) The experimental data from Tripp and Graham¹⁷, on the measured weight gain of samples in 250 Torr of pure oxygen at different temperatures compared with the model predictions. (b) The predicted parabolic constant as a function of temperature is compared with the data of three different works in the literature.¹⁷⁻¹⁹ The porosity in the scale, f_c , was taken to be 0.05 and the pore radius to be 0.5 micron.

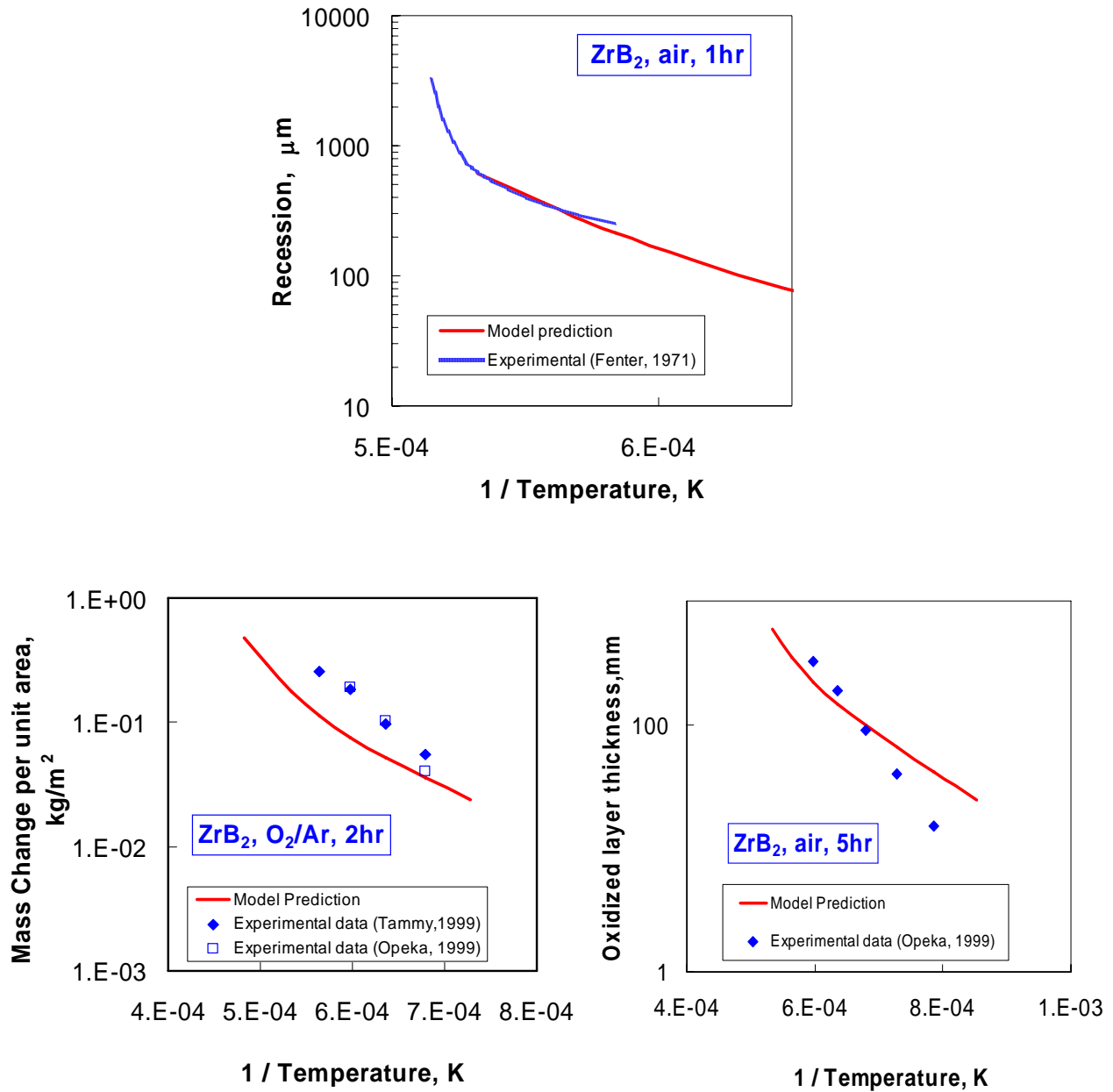


Figure 4 (a) Model predictions of the recession in air as a function of temperature is shown compared with data of Fenter, 1971.⁵ (b) The model predictions for mass change is shown compared with experimental data obtained in Ar/O₂ gas in 2 hrs.^{6,20} (c) The scale thickness obtained after 5hrs in air by Opeka et al.⁶ is shown compared to the predictions. The porosity in the scale, f_c , was taken to be 0.05 and the pore radius to be 0.5 micron.

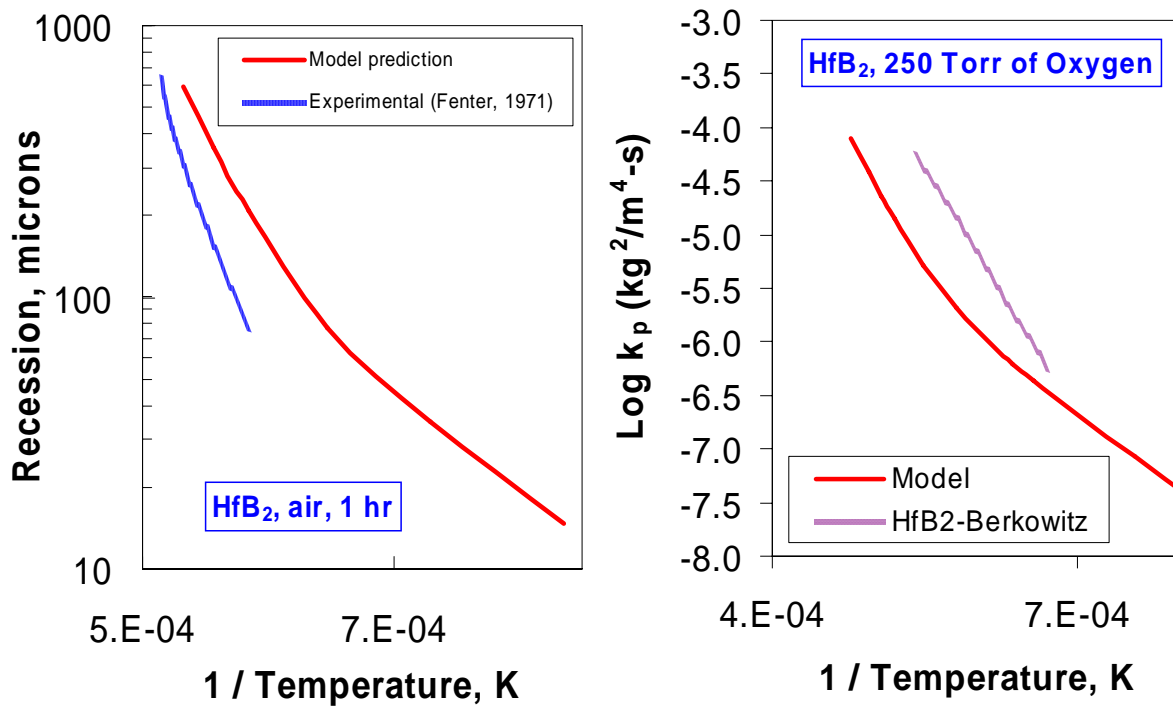


Figure 5 Comparison of model predictions with experimental data on HfB₂.¹⁸ (a) recession in flowing air from Fenter, 1971 and (b) Parabolic constant for weight gain as a function of temperature from Berkowitz, 1966, in 250T of oxygen. The porosity in the scale, f_c , was taken to be 0.05, and pore radius to be 0.5 micron.

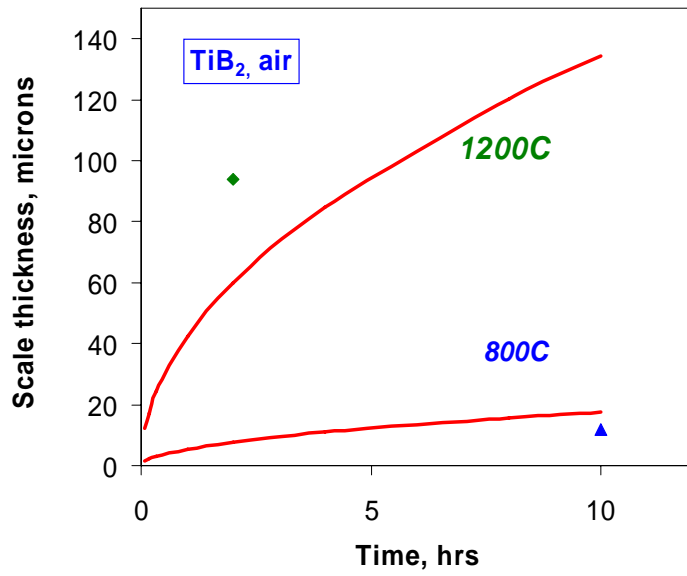
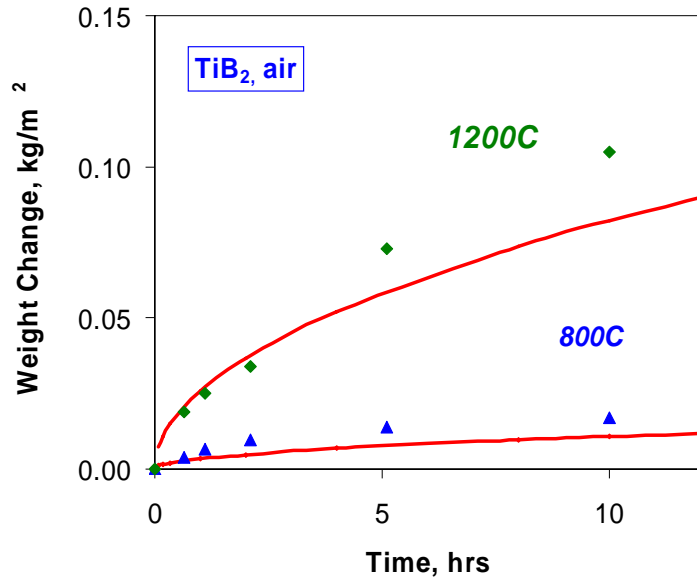


Figure 6 Comparison of model predictions with experimental data on TiB₂. (a) weight gain with time in air and (b) scale thickness after oxidation in air. The porosity in the scale, f_c , was taken to be 0.05, with a pore radius of 0.5 micron. The data were obtained from Koh et al, 2004.²¹

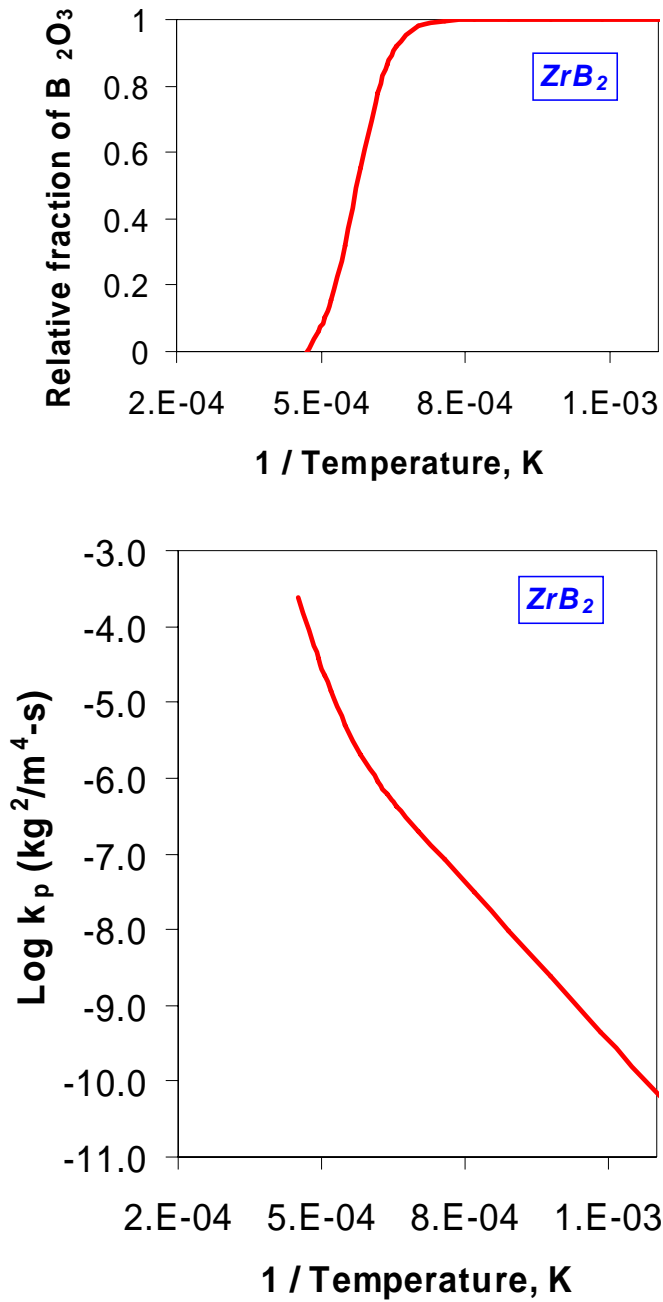


Figure 7 The model predicts a change in the apparent activation energy of the parabolic rate constant that correlates with loss of boron from the scale.

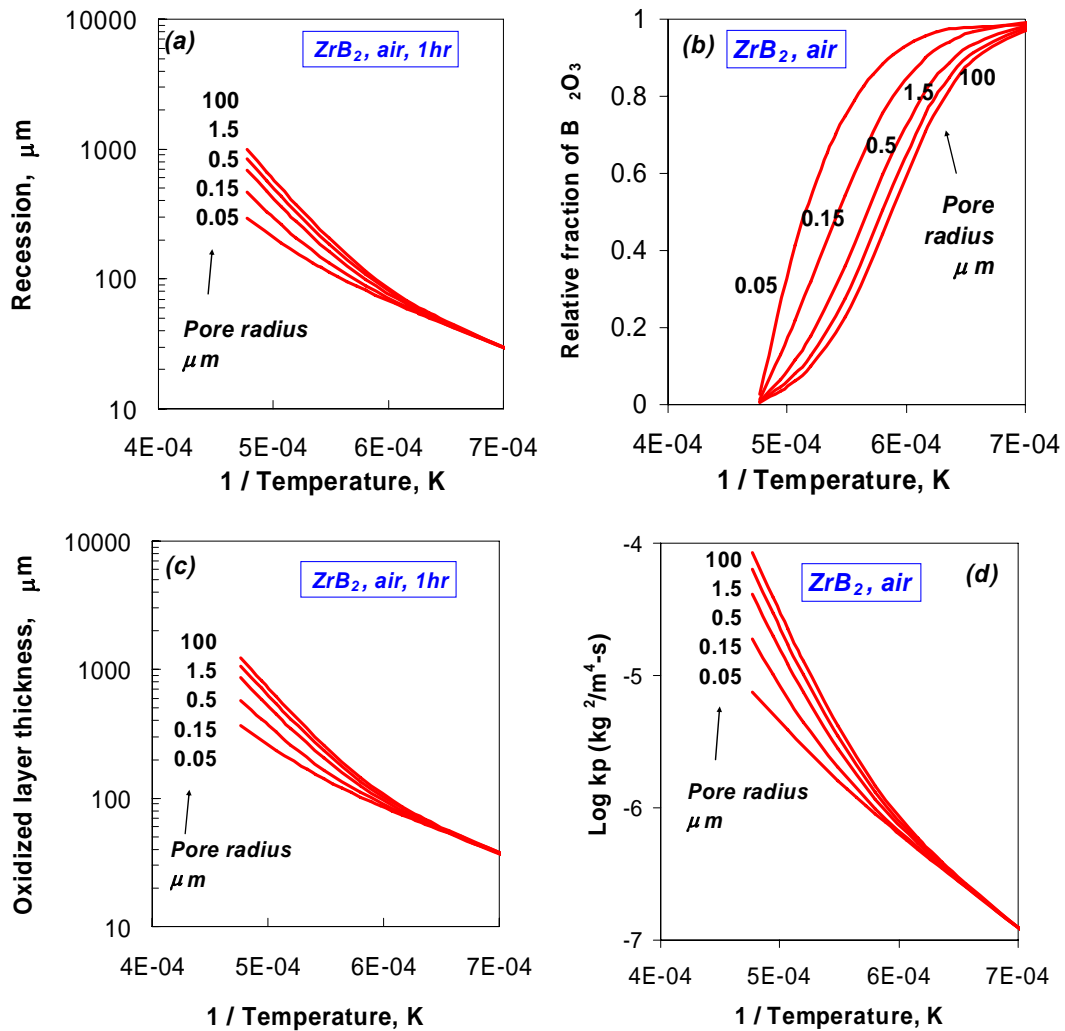


Figure 8 Sensitivity studies show that the pore radius (Knudsen effect) has a significant effect when it is below about 1 micron. The effect on (a) recession, (b) boria fraction in scale, (c) oxide thickness and (d) parabolic rate constant are shown. The effects are insignificant below 1400C, where oxygen diffusion through boria is rate limiting.

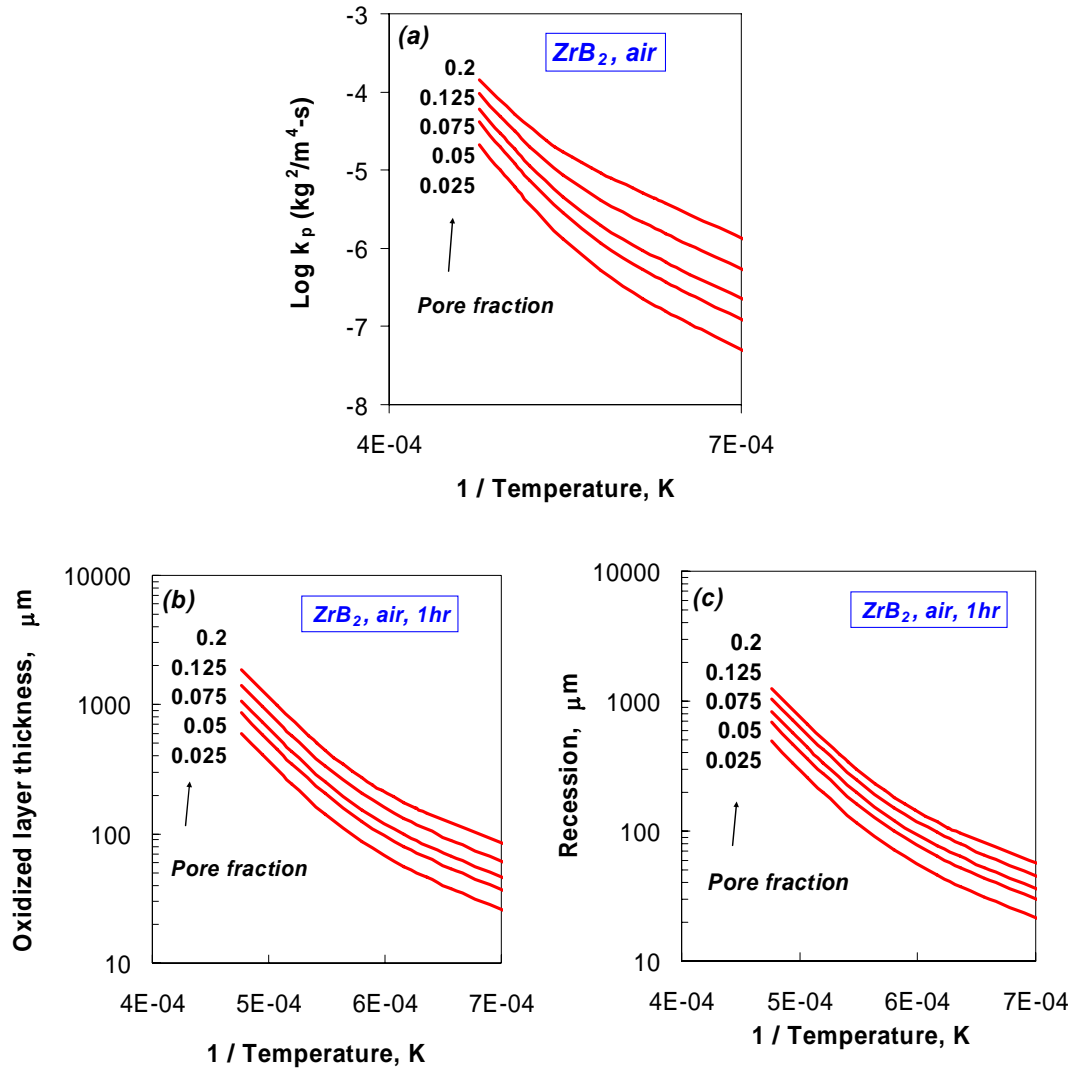


Figure 9 Sensitivity studies show that the effect of pore fraction is nearly linear. It is seen that there is an order of magnitude change in rate constant, oxide thickness and recession, for a change in pore fraction from 0.025 to 0.2.

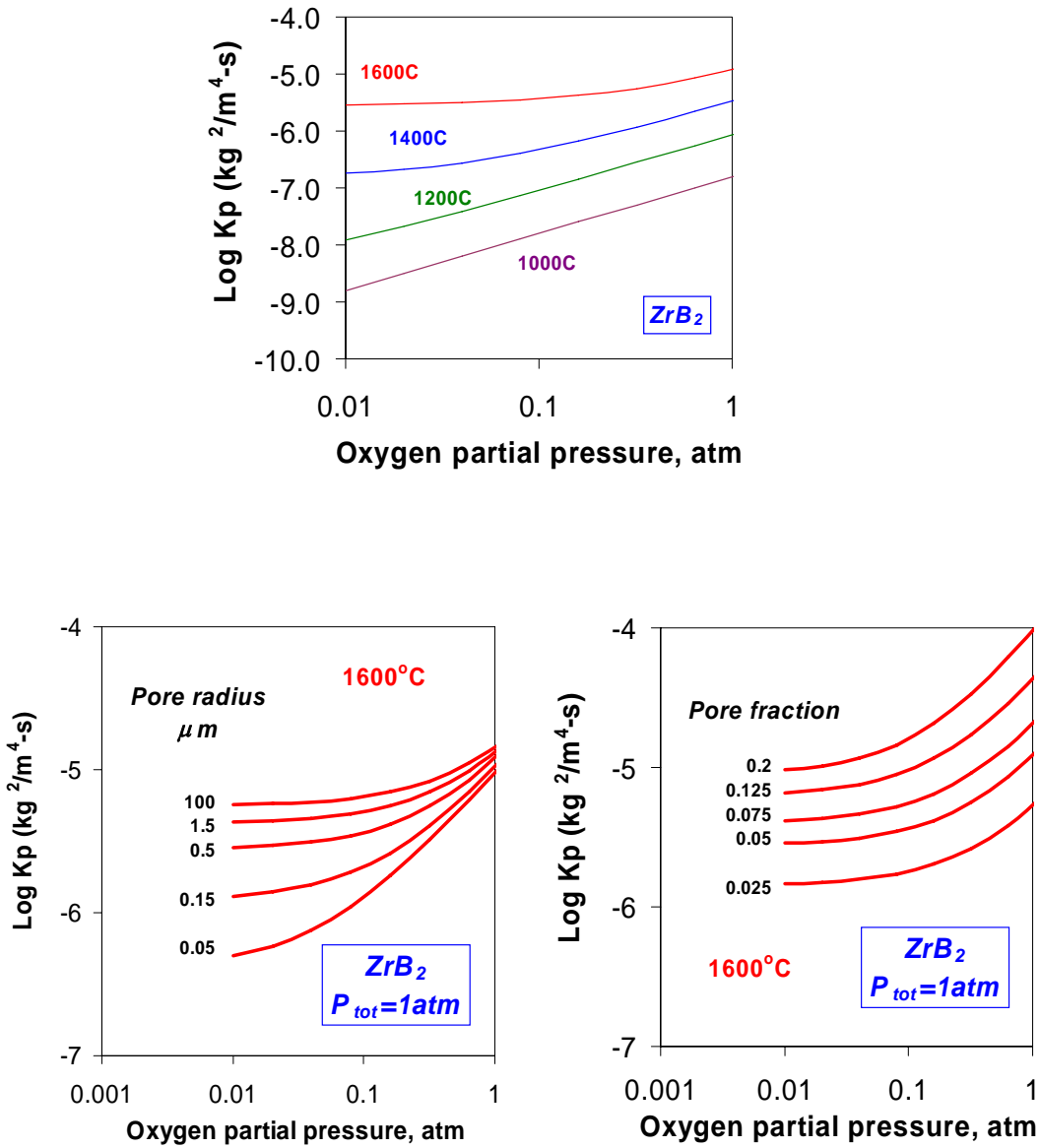


Figure 10. (a) Parametric studies show that the dependence of the parabolic rate constant on the oxygen partial pressure, changes from unity at 1000C to zero above 1600C. The P_{O_2} dependence itself is dependent on (a) the pore size and (b) pore fraction.